Energies **2011**, *4*, 2038-2048; doi:10.3390/en4112038

OPEN ACCESS

energies

ISSN 1996-1073

www.mdpi.com/journal/energies

Article

Water Velocity Measurements on a Vertical Barrier Screen at the Bonneville Dam Second Powerhouse

James S. Hughes *, Z. Daniel Deng *, Mark A. Weiland, Jayson J. Martinez and Yong Yuan

Pacific Northwest National Laboratory, P.O. Box 999, Richland, WA 99352, USA;
E-Mails: Mark.Weiland@pnnl.gov (M.A.W.); Jayson.Martinez@pnnl.gov (J.J.M.);
Yong.Yuan@pnnl.gov (Y.Y.)

* Authors to whom correspondence should be addressed; E-Mails: james.hughes@pnnl.gov (J.S.H.); zhiqun.deng@pnnl.gov (Z.D.D.); Tel.: +1-509-371-6802 (J.S.H.); +1-509-372-6120 (Z.D.D.); Fax: +1-509-371-7160 (J.S.H.); +1-509-372-6089 (Z.D.D.).

Received: 3 August 2011; in revised form: 15 November 2011 / Accepted: 16 November 2011 / Published: 22 November 2011

Abstract: Fish screens at hydroelectric dams help to protect rearing and migrating fish by preventing them from passing through the turbines and directing them towards the bypass channels by means of a sweeping flow parallel to the screen. However, fish screens may actually be harmful to fish if the fish become impinged on the surface of the screen or become disoriented due to poor flow conditions near the screen. Recent modifications to the vertical barrier screens (VBS) in the gate wells at the Bonneville Dam second powerhouse (B2) were intended to increase the guidance of juvenile salmonids into the juvenile bypass system but have resulted in higher mortality and descaling rates of hatchery subyearling Chinook salmon during the 2008 juvenile salmonid passage season. To investigate the potential cause of the high mortality and descaling rates, an *in situ* water velocity measurement study was conducted using acoustic Doppler velocimeters in the gate well slots at turbine units 12A and 14A of B2. From the measurements collected, the average approach velocity, sweep velocity, and the root mean square value of the velocity fluctuations were calculated. The approach velocities measured across the face of the VBS were variable and typically less than 0.3 m/s, but fewer than 50% were less than or equal to 0.12 m/s. There was also large variance in sweep velocities across the face of the VBS with most measurements recorded at less than 1.5 m/s. Results of this study revealed that the approach velocities in the gate wells exceeded criteria intended to improve fish passage conditions that were recommended by National Marine Fisheries Service and the

Washington State Department of Fish and Wildlife. The turbulence measured in the gate well may also result in suboptimal fish passage conditions but no established guidelines to contrast those results have been published.

Keywords: acoustic Doppler velocimetry; fish screen; juvenile bypass system; powerhouse

1. Introduction

Fish screens at water diversion facilities and hydroelectric dams perform a vital function in protecting rearing and migrating fish. Fish screens act as a physical barrier to prevent fish from passing into irrigation canals or turbines and also promote fish movement towards the bypass channels, usually through a sweeping flow parallel to the screen surface [1]. However, the screen itself may be harmful if fish become impinged on the screen surface or become disoriented due to poor flow conditions in close proximity to the screen [2–6]. Therefore, it is critical to understand the hydraulic conditions (e.g., 3-D velocity components, turbulence) that fish encounter upon entering the gate well of a dam's powerhouse. The gate well is the space immediately upstream of the turbine entrance and the collection point for fish diverted upward and away from the primary turbine intake by the guidance structure. Characterizing flows in the gate well will allow for better understanding of the conditions fish experience in the gate well and potentially identify causes of injury and mortality resulting during passage at the dam.

Recent modifications to turbine intakes at Bonneville Dam's second powerhouse (B2) on the Columbia River, in an effort to increase the number of downstream migrating juvenile salmonids guided into the juvenile bypass system (JBS) and away from turbines, have resulted in higher flow velocities into the gate well. A previous laboratory study [7] suggested the modified VBSs installed at B2 could improve flow conditions by establishing a balanced flow distribution through the VBS, yet the study did not predict the high mortality and descaling rate of the hatchery Chinook salmon (*Oncorhynchus tschawytscha*) during the 2008 juvenile salmonid passage season as observed at the Bonneville Dam juvenile monitoring facility (JMF). Because little was known about the hydraulic conditions juvenile salmonids encounter in proximity to the VBS at B2, an *in situ* water velocity measurement study using acoustic Doppler velocimeters (ADV) was conducted in the gate well slots at units 12A and 14A of B2 under varying levels of turbine operation. A 3-D velocity measurement system was developed in order to observe potentially excessive flow velocity components and turbulence present near the VBS. Based on the main findings of the study, this paper provides information that may help explain the high descaling, injury, and mortality of juvenile salmon observed at the Bonneville Dam juvenile fish monitoring facility in 2008.

2. Site Description

Bonneville Dam spans the Columbia River between Oregon and Washington, 234.3 km from the mouth of the Columbia River and approximately 64 km east of Portland, Oregon (Figure 1a). The dam was built and is managed by the United States Army Corps of Engineers, Portland District, and the electrical power generated is distributed by the Bonneville Power Administration. The dam consists of

two powerhouses (B1 and B2), a 442-m-long spillway, and a 206-m-long by 25.9-m-wide navigation lock (Figure 1b). The second powerhouse, located on the north end of the project, has a length of 301 m and consists of eight generators with a total generating capacity of 558 MW. A corner collector, or surface flow outlet, at the south end of B2 (B2CC) was built adjacent to unit 11 in 2004 as a second bypass system for juvenile fish in addition to the existing screened B2 JBS. The VBS's deployed in the gate wells at B2 were designed to allow water that was diverted upward into the gate well to be returned to the turbine intake while preventing fish from doing so (Figure 2).

Figure 1. Bonneville Dam project. (**a**) Location on Columbia River; (**b**) configuration of dam.

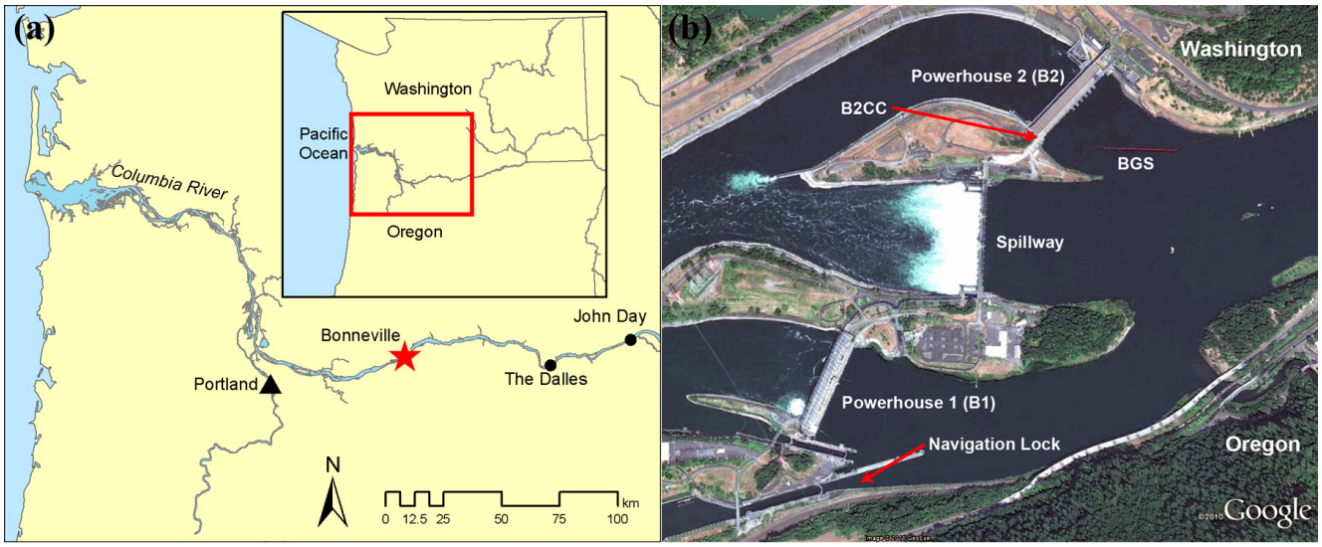

Figure 2. Cross-section view of a gate well slot of B2 intakes. The submerged traveling screen (STS) guides fish from the primary turbine intake flow into the gate well and subsequently into the JBS through the orifice.

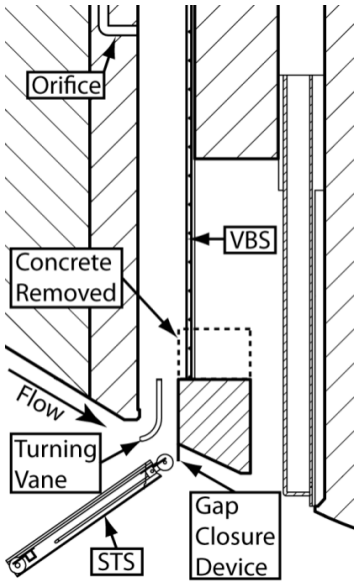

Fish that were entrained in these flows were then passed through an orifice and into the JBS. In recent years, a turning vane and gap closer device have been installed between the submerged traveling

screen (used to guide fish upward into the gate well) and the intake ceiling, resulting in higher flows entering the gate well. To accommodate this increased flow the length of the VBS has been extended downward by the partial removal of a concrete beam that extended the 6.1-m width of the gate well. In addition, the spacing between the vertical stainless steel bars of the VBS was decreased from 0.64 cm to 0.32 cm to abet salmonid fry passage.

3. Methods

3.1. Experimental Setup and Data Collection

The water velocity measurements were conducted in the gate well slots at units 12A and 14A of B2 using two SonTek 5-MHz ADVOcean probes with two SonTek ADVField processor underwater canisters [8]. The SonTek probes and the underwater canisters were mounted to a 5.5-m belt-driven traversing beam (Model HLE 100 SR, Parker Hannifin Corporation, Irwin, PA, USA). The traversing beam was powered by an Empire Magnetics stepper motor (Model WP-U42-42P:10-OFP, Empire Magnetics, Rohnert Park, CA, USA) controlled by a 6K Motion Controller and a ZETA8 micro-stepping driver (Parker Hannifin Corporation, Cleveland, OH, USA). To lower the traversing beam into the gate well slot, two aluminum gantries with electric winches (Model 100AB, My-Te Winch-Hoists, Indianapolis, IN, USA) were placed spanning the width of the gate well slot near each end. To measure the depth of the ADV probes, a fiberglass tape measure was secured to each of the steel winch cables as the traversing beam was lowered into the gate well slot.

The *x*-axis was defined to be perpendicular to the face of the VBS with positive X oriented into the VBS, the *y*-axis was across the width of the gate well slot with positive Y running from north (Washington) to south (Oregon), and the *z*-axis was along the height of the gate well slot with positive Z upward (Figure 3). The origin was at the face of the VBS, the north (Washington) wall of the gate well, and 0 m above sea level.

The two ADV probes were positioned 0.2 m from the upstream face of the VBS, and the measurements covered a depth of approximately 1.8 m above the bottom of the VBS (11.3-m elevation) to 0.6 m above the top of the VBS (17.1-m elevation) with 0.3-m vertical and horizontal increments (Figure 4), resulting in a total of 360 spatial locations covering an area of about 5.8 m by 5.8 m.

Each turbine unit at B2 has three intakes (A, B, and C) with A being the highest flow intake. Flow measurements were carried out in the A gate well of unit 12 (unit 12A) at a unit discharge of 447 m^3/s and in the A gate well of unit 14 (unit 14A) at three unit discharge levels (340, 416, and 447 m^3/s). The levels of discharge selected for testing were all within the 1% operational efficiency curve, as this operational range is most advantageous for maximizing Kaplan turbine output and is standard practice at Bonneville Dam. For each of the scenarios, data sets were obtained with the B2CC opened and closed to examine the effects of the B2CC operational status on the flow field near the VBS. After any change to the unit operations, there was a 30-min break, allowing the flow to normalize before the measurements were continued. During the testing, the average forebay elevation at the B2 powerhouse was 22.6 m above mean sea level with a head differential of 19.2 m.

Figure 3. Coordinate system of the 3-D velocity measurement system (Z-origin is at sea level).

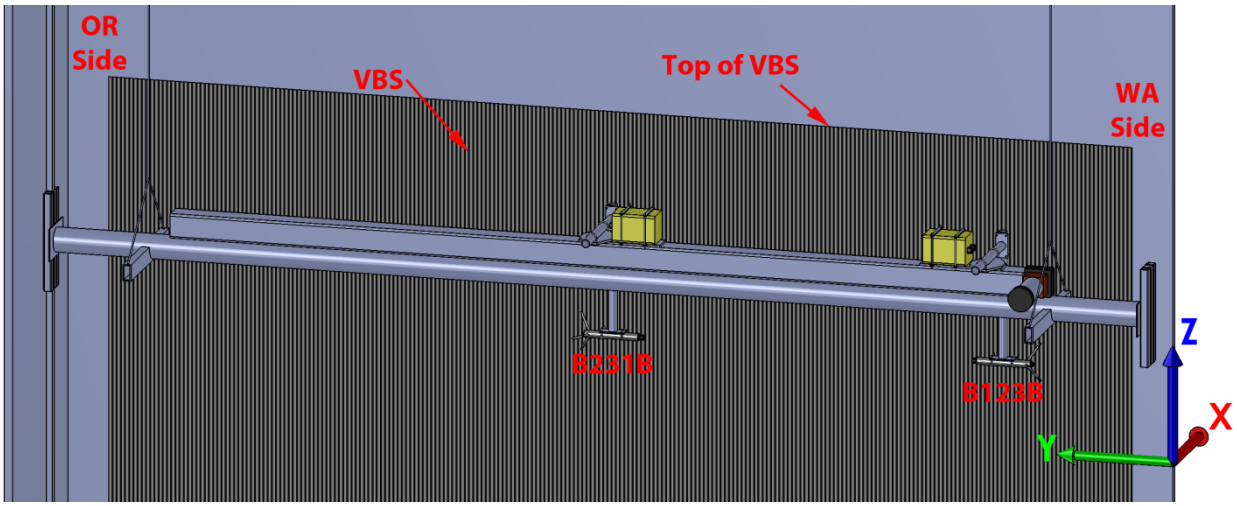

Figure 4. Acoustic Doppler velocimeter probe schematic for measurements taken 0.2 m from the vertical barrier screen.

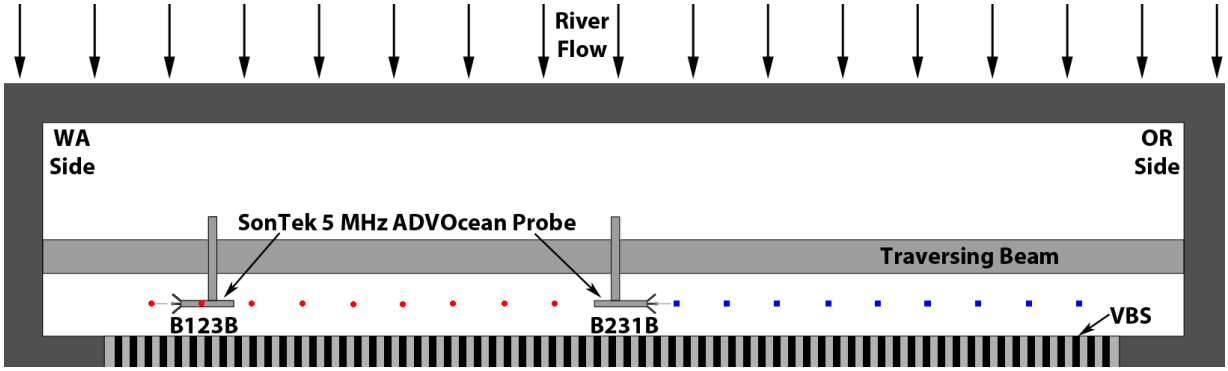

ADV is a common and relatively low-cost tool for turbulence measurements in the field [9–12]. Both ADV systems were operated at a sampling frequency of 25 Hz and were calibrated in a jet flow submerged in a water flume [13]. At each vertical location, the data collection for each ADV system (HorizonADV v1.20, SonTek/YSI, San Diego, CA, USA) and the motion control software (Motion Planner, Parker Hannifin Corporation) that controlled the horizontal locations of the probes were started at approximately the same time. Each horizontal location was sampled for 100 s. Data collection continued as the ADV probes moved between horizontal locations, but data collected during the period of time the ADV probes were moving were not included in the analysis. Following collection of velocity measurements at each depth interval, the data collection for both ADV systems was stopped and the traversing beam manually moved to the next vertical location by using the winches to raise the traversing beam. To account for small differences in the start time of the motion control and the ADV data collection, the first and last 10 s of data at each spatial location were disregarded. This resulted in a total of 80 s of data at each spatial location. Buffin-Bélanger and Roy [14] determined that to capture turbulence statistics from ADV velocity measurements, a data collection time of 60 to 90 s was optimal to provide precise data with minimum sampling effort.

3.2. Data Analysis

Large particles in the water can result in erroneous spikes in velocity measurements recorded by the ADV. To identify and remove the spikes, an acceleration threshold filter was employed [15]. For consecutive velocity measurements, the acceleration of the *n*th sample is given by:

$$A_{i,n} = \frac{V_{i,n} - V_{i,n-1}}{\Delta t} \tag{1}$$

where $i = x$, y, or z and n = sample #.

The acceleration threshold filter calculates the expected minimum and maximum acceleration from the measurements using the parameter λ, which is dependent on the number of samples (N):

$$\lambda = \sqrt{2 \cdot \ln(N)} \tag{2}$$

For a data set consisting of N independent, normally distributed random variables with zero mean and standard deviation, the expected maximum value is given by Equation (3) [16], where the standard deviation of the acceleration is calculated from Equation (4):

$$\text{Max} = \lambda \cdot \sigma \tag{3}$$

where σ is the standard deviation.

$$\sigma_{A_i} = \sqrt{\frac{\sum \left(A_{i,n} - \overline{A}_i \right)^2}{N-1}} \tag{4}$$

where:

$$\overline{A}_i = \frac{\sum A_{i,n}}{N}$$

The first step of applying the acceleration threshold filter is to identify spikes in the acceleration data [17]. A data point is considered a spike if the acceleration is greater than the maximum expected acceleration while the corresponding velocity is greater than the average velocity, or if the acceleration is less than the minimum expected acceleration while the corresponding velocity is less than the average velocity:

$$A_{i,n} > \lambda \cdot \sigma_{A_i} \text{ and } V_{i,n} > \overline{V}_i \tag{5}$$

or:

$$A_{i,n} < -\lambda \cdot \sigma_{A_i} \text{ and } V_{i,n} < \overline{V}_i$$

where:

$$\overline{V}_i = \frac{\sum V_{i,n}}{N}$$

After the spikes in the acceleration data are identified, the second step involves replacing the corresponding velocities with values calculated by linearly interpolating between the nearest two valid points. By replacing the corrupted velocity measurements, the statistical properties on which the

acceleration threshold filter is dependent are changed, and the filtering process is repeated until no additional spikes are detected.

Once the erroneous spikes in the velocity measurements have been removed, the average of the velocity components is calculated from the data points that are not replaced during the filtering process. The average approach velocity ($\bar{V}_a$), which is the component of the flow perpendicular to the face of the VBS, is defined by Equation (6):

$$\bar{V}_a = \bar{V}_x \tag{6}$$

The average sweep velocity ($\bar{V}_s$), which is the component of the flow parallel to the face of the VBS, is calculated using Equation (7):

$$\bar{V}_s = \sqrt{\bar{V}_y^2 + \bar{V}_z^2} \tag{7}$$

The turbulence is quantified using the root mean square (RMS) value of the velocity fluctuations:

$$RMS_i = \sqrt{\frac{\sum\left(V_{i,n} - \bar{V}_i\right)^2}{N}} \tag{8}$$

$$RMS = \sqrt{RMS_x^2 + RMS_y^2 + RMS_z^2}$$

4. Results

Approach velocity and sweep velocity data from individual measurement points were overlaid to illustrate the velocity distribution across the face of the VBS structure at unit 14A during a period when turbine unit discharge was 340 m^3/s with the B2CC open (Figure 5a) and closed (Figure 5b).

Figure 5. Velocity measurements across an area 0.2 m from the face of the VBS at unit 14A, at a turbine unit discharge rate of 340 m^3/s. (**a**) B2CC open; (**b**) B2CC closed.

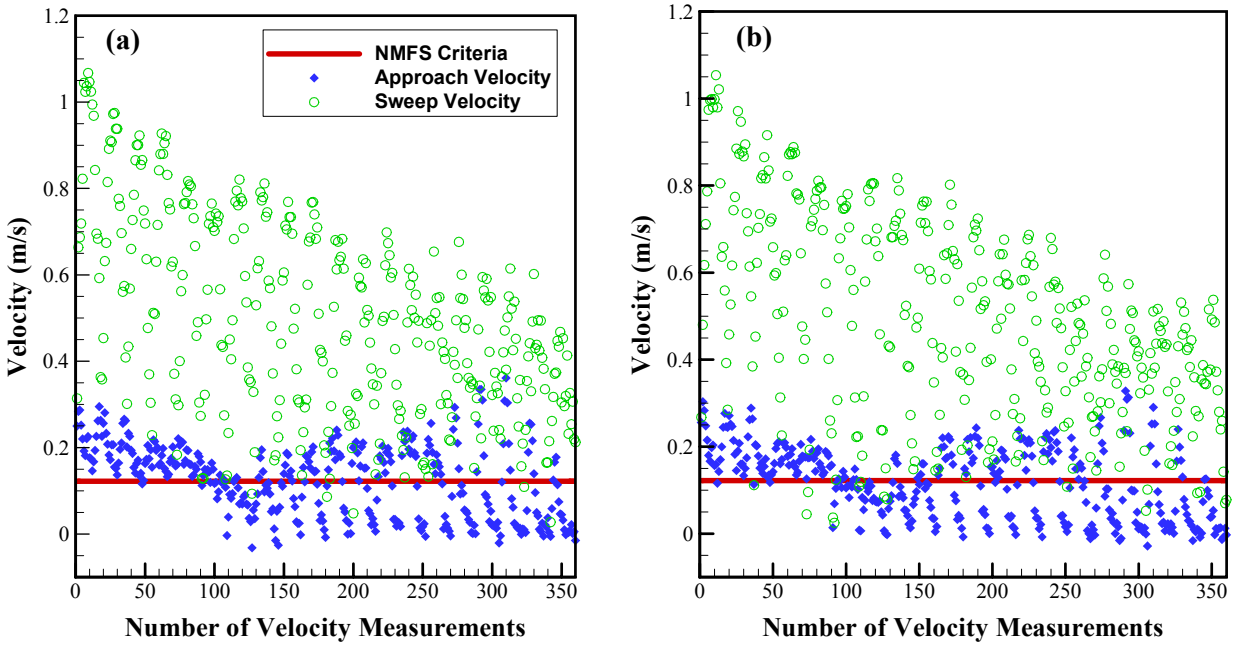

The velocity distributions under different turbine unit discharge rates (416 and 447 m^3/s) exhibit a similar pattern. According to SonTek [8], the accuracy of the velocity measurement is ±0.5 cm/s up to 25 Hz. The approach velocities at each spatial location were used to create contour plots, which were overlaid by a vector field representing the sweep velocity, to illustrate the spatial distribution of the flow at unit 14A when turbine unit discharge was 340 m^3/s with the B2CC open (Figure 6a) and closed (Figure 6b).

Figure 6. Approach velocity contour at unit 14A, at a turbine unit discharge rate of 340 m^3/s. Also shown are sweep velocity vectors in the YZ plane. (**a**) B2CC open; (**b**) B2CC closed.

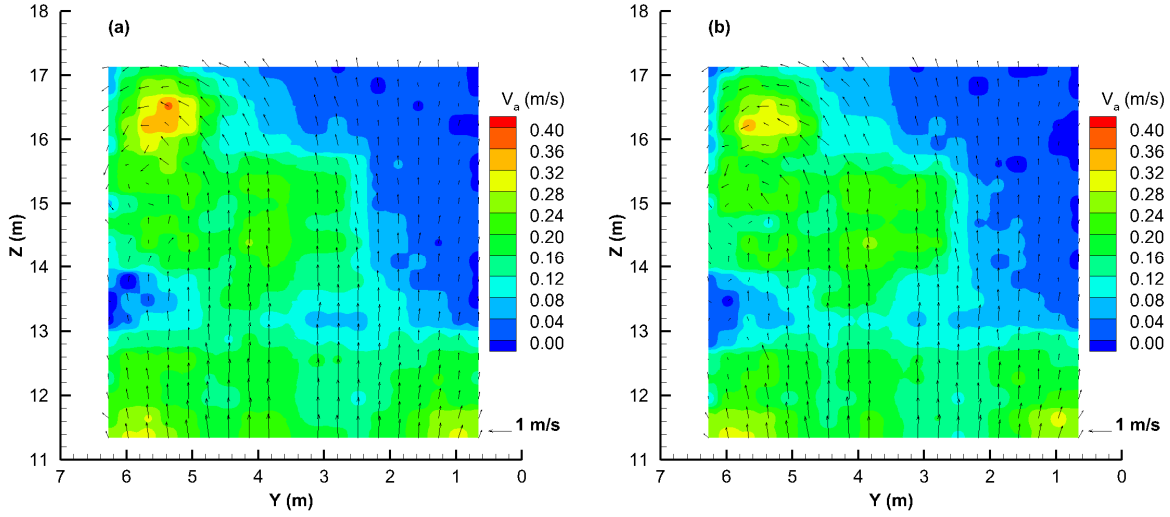

The RMS values of the velocity fluctuations at each spatial location were used to create contour plots to illustrate the spatial distribution of the turbulence at unit 14A when turbine unit discharge was 340 m^3/s with the B2CC open (Figure 7a) and closed (Figure 7b).

Figure 7. RMS velocity fluctuation contour at unit 14A, at a turbine unit discharge rate of 340 m^3/s. (**a**) B2CC open; (**b**) B2CC closed.

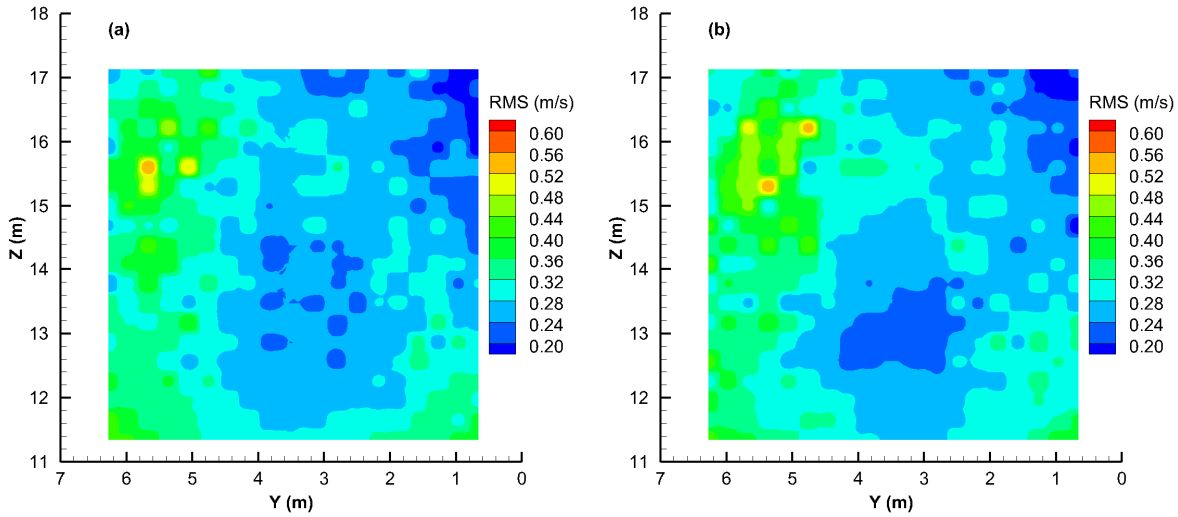

The results were also averaged spatially across the entire measurement area (Table 1) to examine the flow characteristics under different discharge rates and different B2CC operational statuses.

Table 1. Spatially-averaged measurement results for different discharge rates and B2CC operational statuses at units 14A and 12A.

Unit	B2CC Status	Discharge Rate (m^3/s)	V_a (m/s)	% of V_a < 0.12 m/s	V_s (m/s)	RMS (m/s)	V_s/V_a
14A	Open	340	0.126	44.72	0.500	0.292	4.866
	Open	416	0.154	36.39	0.604	0.363	4.707
	Open	447	0.162	35.28	0.627	0.396	4.663
	Closed	340	0.120	48.89	0.491	0.296	5.051
	Closed	416	0.152	36.94	0.610	0.376	4.482
	Closed	447	0.166	33.61	0.664	0.401	4.265
12A	Open	447	0.157	39.72	0.579	0.371	4.466
	Closed	447	0.183	25.00	0.668	0.379	3.938

5. Discussion

National Marine Fisheries Service (NMFS) [18] and the Washington State Department of Fish and Wildlife (WDFW) [19] fish screen criteria provide specific information regarding physical characteristics near the fish screen sites, such as the flow distribution over the screen surface, approach velocities (V_a), and sweep velocities (V_s). A more practical criterion was introduced by McMichael *et al*. [4] to apply to data from the field evaluation of a screen site: 90% of the approach velocity measurements are less than or equal to 0.12 m/s, and the average sweep velocity shall equal or exceed the maximum allowable approach velocity.

The approach velocities varied across the entire face of the VBS but were largely within 0 to 0.3 m/s, with fewer than 50% of the approach velocities less than or equal to 0.12 m/s. All the average approach velocities were more than 0.12 m/s except in one scenario, which occurred in unit 14A at a turbine unit discharge of 340 m^3/s with the B2CC closed. The flow conditions in units 14A and 12A of B2 were not considered to be within the criteria of NMFS or WDFW. In addition, the contour plot of approach velocity and vector plot of sweep velocity indicate the unbalanced flow distribution through the VBS: higher approach velocities occurred at three corners (lower left, lower right, and upper left) of the VBS, while the higher sweep velocities were located at the lower middle portion. Contour plots of the turbulence level represented by the RMS values of the velocity fluctuations demonstrate a similar pattern as the approach velocity is fairly uniform near the center of the VBS with higher values at three corners (lower left, lower right, and upper left) and lower values located at the upper right corner. The sweep velocities showed large variances horizontally (0 to 1.5 m/s), but there was a generally decreasing trend from the bottom of the VBS toward the top. The sweep velocities were generally at least three to four times greater than the approach velocities. This ratio of sweep to approach velocities would meet the sweep velocity criteria set by NMFS or WDFW, as interpreted by [4].

With respect to the turbine unit discharge effects, when the discharge rate increases, the average velocities (approach and sweep) and turbulence also increase. However, the effects of the B2CC operational status on the flow fields were not consistent under the three turbine unit discharge rates. The average approach velocity when the B2CC was open was higher at turbine unit discharge rates of 340 m^3/s and 416 m^3/s and lower at a turbine unit discharge rate of 447 m^3/s; the average sweep velocity when the B2CC was open was higher at a turbine unit discharge rate of 340 m^3/s and lower at

416 m^3/s and 447 m^3/s. The average turbulence was higher at all three turbine unit discharge rates when the B2CC was closed.

Little is known of how migrating juvenile salmonids utilize the gate well slots at Bonneville Dam, other than they must travel nearly the entire vertical length of the VBS (approximately 6 m) to reach the orifice which subsequently allows for passage into the JBS. The uneven distribution of flow across the face of the VBS results in suboptimal passage conditions for migrating fish to include exceedance of the NMFS and WDFW fish screen criteria, stating that no more than 90% of approach velocities should exceed 0.12 m/s. Further investigation is needed to identify potential causes of this unevenly distributed flow and possible structural changes to be made in the gate well.

6. Conclusions

A 3-D velocity measurement system using two ADV probes was developed to investigate the flow conditions in close proximity to the VBS at the Bonneville Dam second powerhouse. This study revealed approach velocities exceeding recommended criteria intended to improve fish passage conditions. Turbulence in the gate well region in proximity to the VBS when the powerhouse was operated at the upper 1% efficiency range may also be expected to result in suboptimal fish passage conditions. These high velocities and turbulent conditions can cause impingement, impact, or descaling of juvenile salmonids before they exit through the orifice into the juvenile fish bypass channel. The powerhouse turbine unit discharge rate directly affected the velocity distribution as well as the turbulence conditions in the gate well. The B2CC operational status had a relatively minor effect (less than 5%) on the velocity and turbulence conditions in the gate well under the three turbine unit discharge rates tested in this study. The uniformity of velocity magnitudes, directions, and variability must be closely monitored, and further VBS improvements are necessary to increase survival and decrease injury rates of fish passing through this portion of Bonneville Dam.

Acknowledgments

The work described in this article was funded by the U.S. Army Corps of Engineers (USACE), Portland District. The study was conducted at Pacific Northwest National Laboratory (PNNL), operated by Battelle for the U.S. Department of Energy. The authors thank Dennis Schwartz, Randy Lee, Jon Rerecich, Ben Hausmann, and Kasey Welch (USACE) and Gene Ploskey, Bob Mueller, Eric Fischer, Geoff McMichael, and Shon Zimmerman (PNNL) for their help with this study.

References

1. Clay, C.H. *Design of Fishways and Other Fish Facilities*; Lewis Publishers: Boca Raton, FL, USA, 1995.
2. Allen, M.E.; Cherian, M.P.; Weber, L.J. Flow through barrier screens—numerical model. In *Proceedings of the North American Water and Environment Congress & Destructive Water*; American Society of Civil Engineers: New York, NY, USA, 1996; pp. 1111–1116.

3. Marmulla, G. *Dams, Fish, and Fisheries: Opportunities, Challenges and Conflict Resolution*; Technical Paper T419; Food and Agriculture Organization of the United Nations: Rome, Italy, 2001.
4. McMichael, G.A.; Vucelick, J.A.; Abernethy, C.S.; Neitzel, D. Comparing fish screen performance to physical design criteria. *Fisheries* **2004**, *7*, 10–16.
5. Swanson, C.; Young, P.S.; Cech, J.J., Jr. Close encounters with a fish screen: integrating physiological and behavioral results to protect endangered species in exploited systems. *Trans. Am. Fish. Soc.* **2005**, *134*, 1111–1123.
6. Rajaratnam, N.; Sadeque, M.A.F.; Katopodis, C. A simple method to predict flow distribution at vertical angled screens in open channels. *Can. J. Civil Eng.* **2006**, *33*, 982–988.
7. ENSR International. *Determine the Backing Plate Porosities and Configuration That Minimizes Velocity Components Normal to the Screen Face for the New VBS Design*; ENSR International: Westford, MA, USA, 2004.
8. SonTek/YSI. *SonTek/YSI ADVField/Hydra: Operation Manual*; SonTek/YSI: San Diego, CA, USA, 2002.
9. Nikora, V.I.; Goring, D.G. ADV measurements of turbulence: Can we improve their interpretation? *J. Hydraul. Eng.* **1998**, *124*, 630–634.
10. Song, T.; Chiew, Y.M. Turbulence measurement in nonuniform open-channel flow using acoustic Doppler velocimeter (ADV). *J. Eng. Mech.* **2001**, *127*, 219–232.
11. García, C.M.; Cantero, M.I.; Niňo, Y.; Garcia, M.H. Turbulence measurements with acoustic Doppler velocimeters. *J. Hydraul. Eng.* **2005**, *131*, 1062–1073.
12. Richmond, M.C.; Deng, Z.; Guensch, G.R.; Tritico, H.; Pearson, W.H. Mean flow and turbulence characteristics of a full-scale spiral corrugated culvert with implications for fish passage. *Ecol. Eng.* **2007**, *30*, 333–340.
13. Deng, Z.; Mueller, R.P.; Richmond, M.C.; Johnson, G.E. Injury and mortality of juvenile salmon entrained in a submerged jet entering still water. *North Am. J. Fish. Manag.* **2010**, *30*, 623–628.
14. Buffin-Bélanger, T.; Roy, A. 1 min in the life of a river: selecting the optimal record length for the measurement of turbulence in fluvial boundary layers. *Geomorphology* **2004**, *68*, 77–94.
15. Cea, L.; Puertas, J.; Pena, L. Velocity measurements on highly turbulent free surface flow using ADV. *Exp. Fluids* **2007**, *42*, 333–348.
16. Donoho, D.L.; Johnstone, I.M. Ideal spatial adaptation by wavelet shrinkage. *Biometrika* **1994**, *81*, 425–455.
17. Goring, D.G.; Nikora, V.I. Despiking acoustic Doppler velocimeter records. *ASCE J. Hydraul. Eng.* **2002**, *128*, 117–126.
18. National Marine Fisheries Service (NMFS). *Juvenile Fish Screen Criteria*; NMFS Environmental & Technical Services Division: Portland, OR, USA, 1996.
19. Washington Department of Fish and Wildlife (WDFW). *Fish Passage Barrier and Surface Water Diversion Screening Assessment and Prioritization Manual*; WDFW: Olympia, WA, USA, 2009.